Structures with Semiactive Variable Stiffness Single/Multiple Tuned Mass Dampers

Satish Nagarajaiah, M.ASCE[1]; and Ertan Sonmez[2]

Abstract: This paper proposes application of single and multiple semiactive variable stiffness tuned mass dampers (STMD/SMTMD) for response control of multistory structures under several types of excitation. A new semiactive control algorithm is developed based on real-time frequency tracking of excitation signal by short time Fourier transform. A parametric study is performed in the frequency domain to investigate the dynamic characteristics and effectiveness of STMDs. Time history responses of single-degree-of-freedom and five-degree-of-freedom structures equipped with STMDs at the roof level, subjected to harmonic, stationary, and nonstationary excitations are presented. STMD/SMTMD are most effective when they have low damping ratios and the excitation frequency can be tracked. They are superior than their passive counterparts in reducing the response of the main structure both under force and base excitations. In case the fundamental frequency changes due to damage or deterioration of the main structure then the TMD will be off-tune; hence, it will lose its effectiveness significantly, whereas, the STMD is robust against such changes as it is always tuned to the excitation frequency.

Introduction

Tuned mass damper (TMD) is a widely used passive energy absorbing device consisting of a secondary mass, a spring, and a viscous damper; it is attached to a primary or main vibratory system to reduce its dynamic motion. TMD was first suggested by Frahm in 1909 (Den Hartog 1985). So its effectiveness depended on the closeness of absorber's natural frequency to the excitation frequency. First closed form expressions for optimum parameters of a TMD were derived by Den Hartog (1985) for an undamped single-degree-of-freedom (SDOF) main structure subjected to harmonic force. Since then, optimum parameters of TMD have been studied extensively. TMD is usually designed by modeling the main structure as an equivalent SDOF structure. McNamara (1977) studied the effectiveness of TMD under wind and white noise excitations, including a 400 t TMD for Citicorp Center (a 274 m high office building). Warburton (1981) studied the optimum parameters of a TMD system with a 2DOF main structure and reported that the parameters determined for 2DOF main structure are in close agreement with the ones for SDOF approximation of the same structure if the ratio of two natural frequencies of the main system is reasonably large. Abe and Igusa (1995)

showed that for multidegree-of-freedom (MDOF) primary structures with widely spaced natural frequencies, the SDOF approximation of the primary structure is the dominant term in the perturbation series and higher order terms can be eliminated by suitably placing several additional TMDs on the structure. Abe and Igusa (1995) also reported that for structures with p closely spaced natural frequencies at least p TMDs are necessary to control the response and derived an analytical condition on the TMD placement that decouples the response of the system onto p SDOF structure/TMD systems. It is well accepted that TMD is effective in reducing the response due to harmonic (Den Hartog 1985) or wind excitations (McNamara 1977). For the seismic effectiveness of TMD, there is no general agreement. Kaynia et al. (1981) and Sladek and Klingner (1983) reported that TMD is not effective in reducing response due to earthquake excitation.

The effectiveness of a TMD is highly dependent to its optimum tuning frequency and optimum damping parameter. Mistuning due to error or change in the natural frequency due to damage/deterioration of the primary structure or off-optimum damping will reduce the efficiency of a TMD significantly. Recently, systems with multiple TMDs (MTMD) have been proposed to eliminate the disadvantages of single TMD systems. Several researchers (Xu and Igusa 1992; Igusa and Xu 1994; Yamaguchi and Harnpornchai 1993) studied the performance and optimum parameters of MTMD systems under harmonic and white noise excitations and showed that optimally designed MTMD system is more effective than the single TMD system. Yamaguchi and Harnpornchai (1993) investigated the fundamental characteristics of MTMD with the parameters of the covering frequency range of MTMD, the damping ratio of each TMD, and the total number of TMDs in comparison to a single TMD for harmonically forced primary structural vibration. Abe and Fujino (1994) reported that a properly designed MTMD can be much more robust than a conventional TMD. Kareem and Kline (1995) studied SDOF systems with MTMD under random loading.

As the conditions of a real primary structural system often change with time due to deterioration or damage, TMD can lose

[1]Professor, Dept. of Civil and Environmental Engineering, and Dept. of Mechanical Engineering and Material Science, Rice Univ., 6100 S. Main St., Houston, TX 77005. E-mail: nagaraja@rice.edu

[2]Graduate Student, Dept. of Civil and Environmental Engineering, Rice Univ., 6100 S. Main St., Houston, TX 77005. E-mail: sonmeze@rice.edu

effectiveness due to mistuning. In a recent application of TMD in a tower in Canada mistuning occurred due to damage in shear walls of the tower rendering the TMD ineffective. The need for adaptivity and retuning has led to development of semiactive TMD (STMD) and active TMD (ATMD). Efforts are underway to retrofit the tower/TMD in Canada; however, a STMD would have retuned itself and continued to be effective by retuning to the new main structure (tower) frequency, which has been demonstrated by Nagarajaiah and Varadarajan (2005) and Varadarajan and Nagarajaiah (2004).

An extensive survey of passive, semiactive, and active TMDs has been presented by Sun et al. (1995). The main advantage of STMD is response reduction comparable to an ATMD, but with an order of magnitude less power consumption (Nagarajaiah and Varadarajan 2005). STMDs have been investigated by Hrovat et al. (1983), Abe (1996), and Abe and Igusa (1996). Several variable damping devices, such as magnetorheological, variable orifice, and electrorheological dampers have been developed (Spencer and Nagarajaiah 2003). Variable stiffness systems, with either on or off states, have been developed by Kobori and Takahashi (1993), Bobrow et al. (2000), and Yang et al. (2000). A new semiactive independently variable stiffness (SAIVS) device has been developed by Nagarajaiah and Mate (1998) and studied by Nagarajaiah et al. (1999). Using this device a new semiactive variable stiffness TMD has been developed by Nagarajaiah and Varadarajan (2000). The STMD has the distinct advantage of continuously retuning its frequency in real time, thus making it robust to changes in primary system stiffness and damping. Recently, the STMD device has been studied by developing on-line tuning using empirical mode decomposition-Hilbert transform and short-time Fourier transform (STFT) algorithms by Varadarajan and Nagarajaiah (2004) and Nagarajaiah and Varadarajan (2005), which tune the frequency of STMD and reduce the primary structural response; it has been shown that STMD is effective in reducing wind induced response of buildings (i.e., main structure) and is robust against changes in building stiffness.

In this paper application of single and multiple semiactive variable stiffness tuned mass dampers (STMD/SMTMD) to reduce the response of the main structure under several type of excitations is proposed. A new semiactive control algorithm is developed based on real-time frequency tracking of excitation signal by short-time Fourier transform (STFT). It is shown that frequencies of simple harmonic signals can be tracked accurately using STFT. Based on this result, a parametric study is performed in the frequency domain to investigate the dynamic characteristics and effectiveness of STMDs. Time history responses of SDOF and five-degree-of-freedom (5DOF) main structures equipped with STMDs at the roof level, subjected to harmonic, stationary, and nonstationary excitations are presented. STMD/SMTMD are most effective when they have low damping ratios and the excitation frequency can be tracked accurately. They are superior than their passive counterparts in reducing the response of the main structure both under force and base excitations. In case the fundamental frequency changes due to damage or deterioration of the main structure then the TMD will be off-tune; hence, it will lose its effectiveness significantly, whereas, the STMD is robust against such changes since it is always tuned to the excitation frequency.
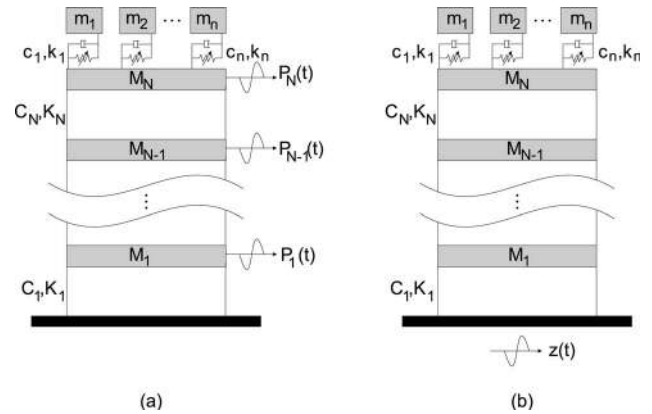

Fig. 1. MDOF structural model with SMTMD (varying $k_1, \ldots, k_n$) at the roof level: (a) force excited; (b) base excited

Modeling of MDOF System with MTMD

The main structure is modeled as a regular multistory shear building in which the structural properties (stiffness and damping) of each story are uniform. The model of N-story building with n-TMD at the roof is presented in Fig. 1. The frequencies of the n-TMD are distributed around the natural frequency of the main structure, as shown in Fig. 2. Several definitions and assumptions made in this study are listed as follows:

- The main structure is symmetric and has uniform mass ($M_1 = \cdots = M_N = M_0$), stiffness ($K_1 = \cdots = K_N = K_0$) and stiffness-proportional damping ($C_1 = \cdots = C_N = C_0$) properties throughout its height. $\omega_0 = \sqrt{K_0/M_0}$ and $\zeta_0 = C_0/(2M_0\omega_0)$ = parameters chosen such that the first mode frequency and damping ratio of the main structure have the desired values. First modal damping ratio of the main structure is 1% ($\zeta_{n1} = 0.01$). Only SDOF ($N=1$) and 5DOF ($N=5$) models of main structure are considered for simulations, without loss of generality.
- TMDs are modeled as SDOF systems with same mass ($m_1 = \cdots = m_n = m_0$), damping ratio ($\xi_1 = \cdots = \xi_n = \xi_0$) but different stiffness ($k_j : j = 1, 2, \ldots, n$) properties.
- γ_j is defined as the frequency of jth TMD ($\omega_j = \sqrt{k_j/m_j}$) normalized by first natural frequency of the main structure (ω_{n1}); $\gamma_c = \omega_c/\omega_{n1}$ = normalized frequency of the central TMD (ω_c = frequency of central TMD); $\gamma_0 (=\gamma_c - 1)$ = offset of the central frequency of the MTMD from the natural frequency of the main structure; and $\Delta\gamma$ = normalized frequency range of the MTMD.
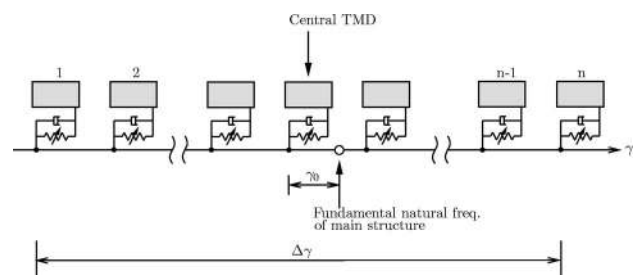

Fig. 2. Frequency distribution of SMTMD

- Each TMD has a slightly different damping coefficient depending on ω_j (i.e., $c_j = 2m_0\omega_j\xi_j$).
- Total mass ratio ($\mu = \Sigma_1^n m_0 / \Sigma_1^N M_0$) is fixed to 1% such that jth TMD mass ratio, μ_j is equal to $0.01/n$ in an n-TMD system.
- The optimum frequency ratio γ_{opt} and damping ratio ξ_{opt} for TMD in a SDOF structure is obtained numerically using frequency response functions. The central frequency of MTMD is set to the same frequency of the single TMD; then optimum frequency range and individual TMD damping ratio are computed numerically. In 5DOF structure, TMD and MTMD are designed with respect to first mode properties of the 5DOF structure ($\mu = 0.0159$).

Modeling of MDOF System with SMTMD

There are several semiactive variable stiffness devices that are proposed and studied in the literature. As described earlier the SAIVS device has been developed by and patented [S. Nagarajaiah, "Structural vibration damper with continuously variable stiffness," U.S. Patent No. 6,098,969 (2000)] with capability to continuously and independently vary stiffness. The SAIVS device, shown in Fig. 3, consists of four spring elements arranged in a plane rhombus configuration with pivot joints at the vertices. A linear electromechanical actuator configures the aspect ratio of the rhombus configuration of SAIVS device. The aspect ratio changes between the fully closed (Joints 1 and 2 are in closest position) and open configurations (Joints 3 and 4 are in closest position) leading to maximum and minimum stiffness, respectively. A control algorithm and controller are used to regulate the linear electromechanical actuator. The power required by the actuator to change the aspect ratio of the device is nominal. The variable stiffness of the SAIVS device is described by

$$k(t) = k_e \cos^2[\theta(t)] \qquad (1)$$

where $k(t) =$ time varying stiffness of the device, $k_e =$ constant spring stiffness of each spring element; and $\theta(t) =$ time varying angle of the spring elements with the horizontal in any position of the device. The SAIVS device has maximum stiffness in its fully closed [$\theta(t) = 0$] and minimum stiffness in its fully open position [$\theta(t) \sim \pi/2$]. The device can be positioned in any configuration, changing its stiffness continuously, independently, and smoothly between maximum and minimum stiffness.

The previous assumptions and definitions made for TMD and MTMD are also same for STMD and SMTMD except that in the semiactive case central TMD is tuned to excitation frequency [$\omega(t)$] such that $\gamma_c(t) = \omega(t)/\omega_{n1}$. In each STMD, damping coeffi-

Fig. 3. SAIVS device

cient is constant and damping ratio varies with time due to varying tuning frequency [$c_j = 2\xi_j(t)\omega_j(t)m_0$]. For convenience damping coefficient is defined with respect to selected reference damping ratio ($\xi_j^{ref} = \xi^{ref}$) and corresponding passive TMD frequency (ω_j^p) such that $c_j = 2\xi_j^{ref}\omega_j^p m_0 = 2\xi_j(t)\omega_j(t)m_0$. Time dependent damping ratio can be obtained as $\xi_j(t) = c_j/[2\omega_j(t)m_0]$ or $\xi_j(t) = \xi_j^{ref}\omega_j^p/\omega_j(t)$. For ease of presenting and interpreting the results, STMDs are parameterized with respect to reference damping ratio, which corresponds to the damping ratio when STMD is tuned to the same frequency of corresponding passive TMD.

Formulation

The equations of motion for the structural model given in Fig. 1 can be written as follows:

$$\mathbf{M\ddot{X}} + \mathbf{C\dot{X}} + \mathbf{KX} = \mathbf{P}(t) \qquad (2)$$

where $\mathbf{X} = \{X_1\ X_2\ \cdots\ X_N\ x_1\ x_2\ \cdots\ x_n\}^T =$ displacement vector in which $X_i =$ displacement of ith story; $x_j =$ displacement of jth TMD; and $\mathbf{P}(t) =$ force vector. The coefficient matrices in Eq. (2) are the mass, damping, and stiffness matrices defined as

$$\mathbf{M} = \begin{bmatrix} M_1 & 0 & \cdots \\ 0 & M_2 & 0 & \cdots \\ \vdots & 0 & \ddots & \ddots \\ & \vdots & \ddots & M_N \\ & & & & m_1 & 0 & \cdots \\ & & & & 0 & m_2 & \ddots \\ & & & & \vdots & \ddots & \ddots \\ & & & & & & & m_n \end{bmatrix} = M_0 \begin{bmatrix} \mathbf{I} & \mathbf{0} \\ \mathbf{0} & \mu_0\mathbf{I} \end{bmatrix} = M_0\mathbf{\bar{M}} \qquad (3)$$

$$
\mathbf{C} = \begin{bmatrix} \begin{bmatrix} C_1 + C_2 & -C_2 & 0 & \cdots & & \\ -C_2 & C_2 + C_3 & -C_3 & \ddots & & \\ 0 & -C_3 & C_3 + C_4 & \ddots & & \\ \vdots & \ddots & \ddots & \ddots & -C_{N-1} & \\ & & & -C_{N-1} & C_N \end{bmatrix} + \begin{bmatrix} \sum\limits_{j=1}^{n} c_j & -c_1 & -c_2 & \cdots & -c_n \\ -c_1 & c_1 & 0 & \cdots & 0 \\ -c_2 & 0 & c_2 & \ddots & \vdots \\ \vdots & \vdots & \ddots & \ddots & \\ -c_n & & & & c_n \end{bmatrix} \end{bmatrix} = C_0 \bar{\mathbf{C}} \tag{4}
$$

$$
\mathbf{K} = \begin{bmatrix} \begin{bmatrix} K_1 + K_2 & -K_2 & 0 & \cdots & & \\ -K_2 & K_2 + K_3 & -K_3 & \ddots & & \\ 0 & -K_3 & K_3 + K_4 & \ddots & & \\ \vdots & \ddots & \ddots & \ddots & -K_{N-1} & \\ & & & -K_{N-1} & K_N \end{bmatrix} + \begin{bmatrix} \sum\limits_{j=1}^{n} k_j & -k_1 & -k_2 & \cdots & -k_n \\ -k_1 & k_1 & 0 & \cdots & 0 \\ -k_2 & 0 & k_2 & \ddots & \vdots \\ \vdots & \vdots & \ddots & \ddots & \\ -k_n & & & & k_n \end{bmatrix} \end{bmatrix} = K_0 \bar{\mathbf{K}} \tag{5}
$$

where $\bar{\mathbf{M}}$, $\bar{\mathbf{C}}$, and $\bar{\mathbf{K}}$ = normalized mass, damping, and stiffness matrices and $\mu_0 = m_0/M_0$. The force vector is defined for force and base excitations as

$$
\mathbf{P(t)} = \begin{cases} \bar{\mathbf{P}}p(t) = \bar{\mathbf{P}}p_0\bar{p}(t) & \text{(force excited)} \\ -\mathbf{M}\mathbf{1}\ddot{z}(t) = -M_0\bar{\mathbf{M}}\mathbf{1}\ddot{z}_0\bar{\ddot{z}}(t) & \text{(base excited)} \end{cases} \tag{6}
$$

A reference response value, $X_{0,\text{st}}$ is defined as $X_{0,\text{st}} = p_0/K_0$ for force excitation and $X_{0,\text{st}} = M_0\ddot{z}_0/K_0$ for base excitation. Substituting $X_{0,\text{st}}$ in Eq. (2) gives

$$
\bar{\mathbf{M}}\ddot{\mathbf{X}} + 2\zeta_0\omega_0\bar{\mathbf{C}}\dot{\mathbf{X}} + \omega_0^2\bar{\mathbf{K}}\mathbf{X} = \begin{cases} \omega_0^2 X_{0,\text{st}}\bar{\mathbf{P}}\bar{p}(t) & \text{(force excited)} \\ -\omega_0^2 X_{0,\text{st}}\bar{\mathbf{M}}\mathbf{1}\bar{\ddot{z}}(t) & \text{(base excited)} \end{cases} \tag{7}
$$

Dividing $\mathbf{X}$, $\dot{\mathbf{X}}$, and $\ddot{\mathbf{X}}$ by $X_{0,\text{st}}$ leads to the normalized equations of motion as

$$
\bar{\mathbf{M}}\bar{\ddot{\mathbf{X}}} + 2\zeta_0\omega_0\bar{\mathbf{C}}\bar{\dot{\mathbf{X}}} + \omega_0^2\bar{\mathbf{K}}\bar{\mathbf{X}} = \begin{cases} \omega_0^2\bar{\mathbf{P}}\bar{p}(t) \\ -\omega_0^2\bar{\mathbf{M}}\mathbf{1}\bar{\ddot{z}}(t) \end{cases} \tag{8}
$$

Eqs. (7) and (8) can be solved by Newmark's method to obtain the actual or normalized response, respectively.

The aforementioned formulation can also be specified in state space in the form

$$
\dot{\chi} = \mathbf{A}\chi + \mathbf{A}_s(t)\chi + \mathbf{BF} \tag{9}
$$

where $\chi = [\mathbf{X}\ \dot{\mathbf{X}}]^T$ = state vector; $\mathbf{A}$ = time-independent state matrix (corresponding to passive properties); $\mathbf{A}_s(t)$ = time-dependent state matrix (corresponding to semiactive properties); $\mathbf{B}$ = input coupling matrix; and $\mathbf{F}$ = input force vector.

Results

Excitation Frequency Tracking by STFT

The STFT is one of the most popular methods for studying nonstationary signals. The basic idea of STFT is: to break up the signal into small-time segments and Fourier analyze each time segment to identify the frequencies that existed in that segment. The totality of such spectra describes how the spectrum is varying in time (Cohen 1995). Mathematically, the short-time Fourier transform can be described by

$$
\text{STFT}(t,\omega) = S(t,\omega) = \int s(\tau)w(\tau - t)e^{-j\omega\tau}d\tau \tag{10}
$$

where $s(t)$ = signal and $w(\tau - t)$ = window function which is chosen to leave the signal more or less unaltered around the time t but to suppress the signal for times distant from the time of interest. The instantaneous (or dominant) frequency of the excitation signal at discrete time t_i is computed by

$$
f_{\text{inst}}(t_i) = \frac{\sum\limits_{k=\max(1,i-m+1)}^{i} f_{\text{inst}}(t_k)\max[|S(t_k,f)|^2]}{\sum\limits_{k=\max(1,i-m+1)}^{i} \max[|S(t_k,f)|^2]} \tag{11}
$$

where m = number of points used for averaging; and f = cyclic frequency (Hz).

The block diagram for control algorithm is given in Fig. 4. Note that the feedback shown in Fig. 4 is only for adjusting the proper positioning of semiactive device. Further details in implementation of frequency tracking and tuning of STMD are shown
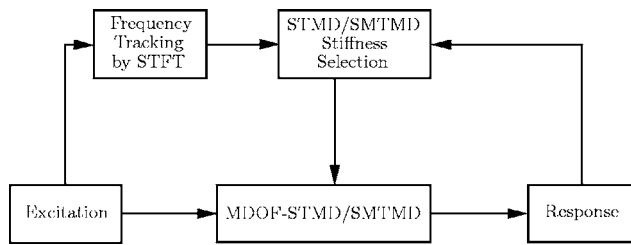
Fig. 4. Control algorithm

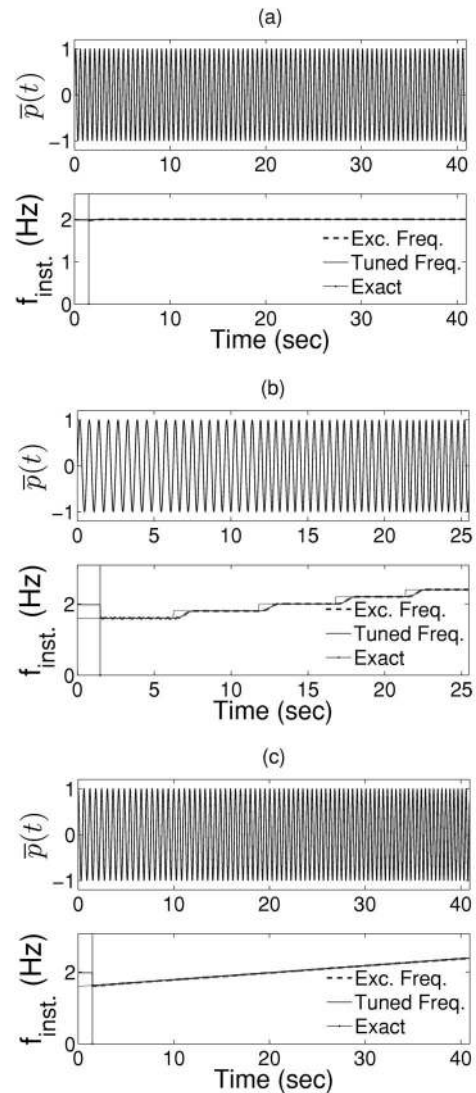**Fig. 6.** Frequency tracking for (a) harmonic sinusoidal; (b) discrete sinusoidal sweep; and (c) linear chirp

in Fig. 5. The procedure starts by selecting a STFT window and a window length (WL) of $n\Delta t$ ($n+1$=number of points in the window). Time lapse (TL) of $L\Delta t$=time period between successive windows. The signal is convolved with window function, $w(\tau)$ and then zero padded for the desired frequency resolution. Fast Fourier transform (FFT) power spectrum of each window is calculated and dominant excitation frequency is determined using Eq. (11) by weighting the dominant frequency by its maximum FFT power at the corresponding time. Averaging length, AL=$m\Delta t$=time length considered in weighted averaging of dominant frequency and t_0=time required before starting to tune STMDs to ensure sufficient number of signal points are collected for FFT calculation. Once $t > t_0$, dominant frequency is checked if it is satisfying the lower and upper frequency limits ($f_{\text{lim}1}$ and $f_{\text{lim}2}$). If it is within lower and upper bounds, STMD is tuned to dominant frequency; if it is not within the bounds or $t < t_0$, STMD is tuned to optimum passive TMD frequency.

Three kinds of harmonic signals and their frequency tracking are shown in Fig. 6. The first signal is harmonic sinusoidal with 2 Hz frequency, the second signal is discrete sinusoidal sweep with consecutive ten cycles of five frequencies (1.6, 1.8, 2.0, 2.2, and 2.4 Hz) and the third signal is a linear chirp with frequencies varying from 1.6 to 2.4 Hz continuously. A rectangular window with a length of WL=2 s, TL=Δt=0.02 s, AL=1 s, and t_0=1.5 s are used to track the harmonic sinusoidal signal; for the discrete sinusoidal sweep and linear chirp signal the parameters are selected as WL=1 s, TL=Δt=0.02 s, AL=0.5 s, and t_0=1.5 s. It is clear from Fig. 6 that such signals can be tracked satisfactorily.
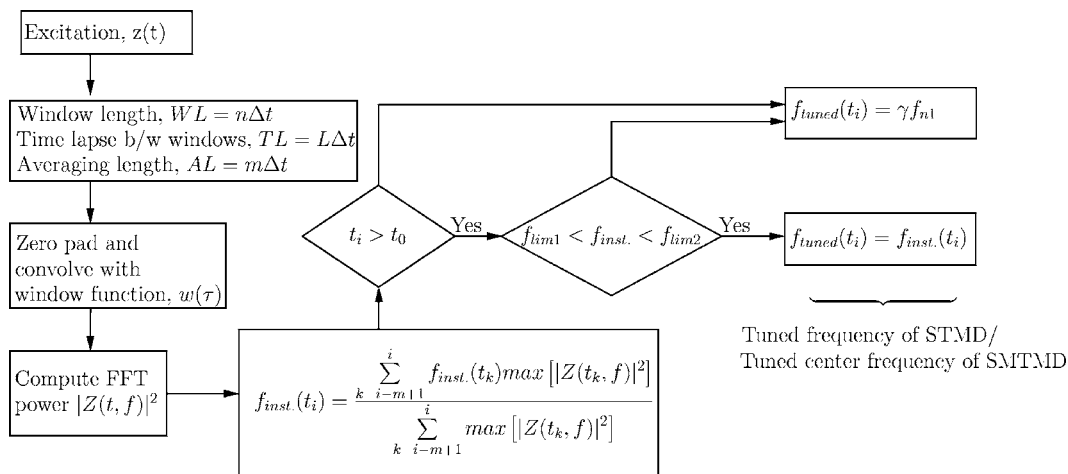
Fig. 5. Frequency tracking by STFT and STMD/SMTMD tuning

Parametric Study

In order to study the parameters governing STMD/SMTMD systems, the main structure is considered as a SDOF system (representing the fundamental mode of a MDOF system). Thus, parameters ω_0 and ζ_0 become natural frequency ω_n, and damping ratio ζ_n of the main structure, respectively. The excitation is limited to harmonic loading and it is assumed that the exact excitation frequency is known or can be tracked as in Fig. 6. Defining the excitation as a complex harmonic function such that $\bar{p}(t) = e^{i\omega t}$, $\bar{\bar{z}}(t) = e^{i\omega t}$, Eq. (8) becomes

$$\bar{\mathbf{M}}\bar{\bar{\mathbf{X}}} + 2\zeta_n\omega_n\bar{\mathbf{C}}\bar{\bar{\mathbf{X}}} + \omega_n^2\bar{\mathbf{K}}\bar{\mathbf{X}} = \begin{cases} \omega_n^2\bar{\mathbf{P}}e^{i\omega t} \\ -\omega_n^2\bar{\mathbf{M}}\mathbf{1}e^{i\omega t} \end{cases} \quad (12)$$

Assuming a harmonic solution as

$$\bar{\mathbf{X}} = \mathbf{\Phi}e^{i\omega t} \quad (13)$$

Substituting force and solution expressions above into equations of motion leads to

$$(-\omega^2\bar{\mathbf{M}} + 2\zeta_n\omega_n i\omega\bar{\mathbf{C}} + \omega_n^2\bar{\mathbf{K}})\mathbf{\Phi} = \begin{cases} \omega_n^2\bar{\mathbf{P}} \\ -\omega_n^2\bar{\mathbf{M}}\mathbf{1} \end{cases} \quad (14)$$

The magnitude of frequency response functions can be obtained by
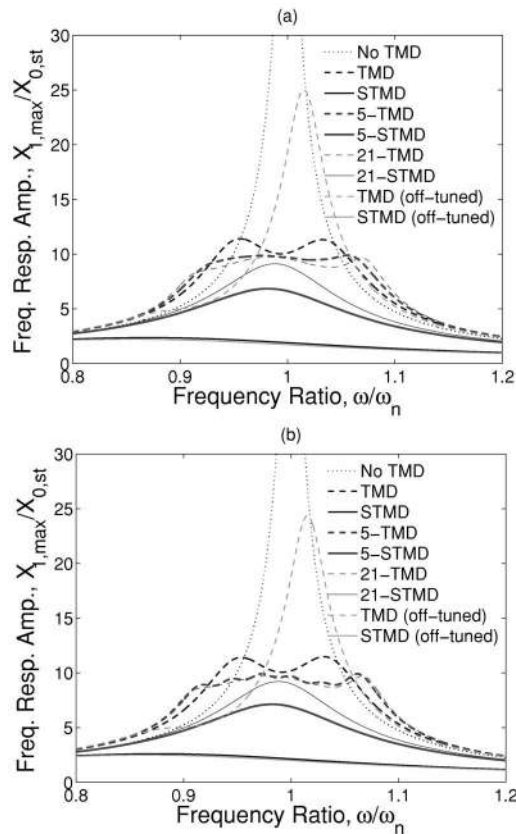
Fig. 7. Frequency response amplitudes of SDOF main structure ($\zeta_n = 0.01$) for no TMD, TMD, MTMD, STMD, and SMTMD ($\mu = 0.01$): (a) force excitation; (b) base excitation
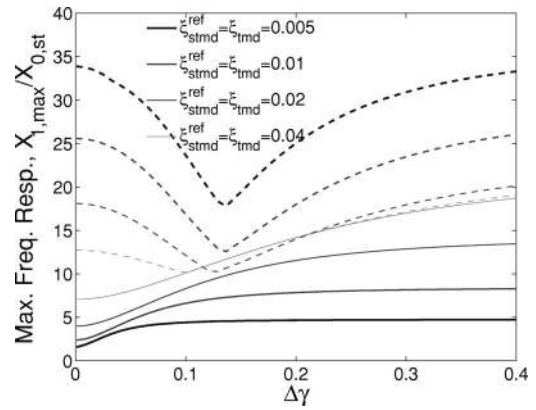
Fig. 8. Maximum frequency response versus MTMD frequency range for force excited SDOF with 5TMD (dashed line)/5STMD (solid line)

$$\left|\mathbf{\Phi}\left(\frac{\omega}{\omega_n}\right)\right| = \begin{cases} \left|\left[-\left(\frac{\omega}{\omega_n}\right)^2\bar{\mathbf{M}} + 2\zeta_n\left(\frac{\omega}{\omega_n}\right)i\bar{\mathbf{C}} + \bar{\mathbf{K}}\right]^{-1}\bar{\mathbf{P}}\right| \\ \left|-\left[-\left(\frac{\omega}{\omega_n}\right)^2\bar{\mathbf{M}} + 2\zeta_n\left(\frac{\omega}{\omega_n}\right)i\bar{\mathbf{C}} + \bar{\mathbf{K}}\right]^{-1}\bar{\mathbf{M}}\mathbf{1}\right| \end{cases} \quad (15)$$

The frequency response amplitudes of force excited and base excited SDOF are presented in Figs. 7(a and b) for several passive and semiactive cases. The optimum frequency, damping ratio, and frequency range of passive TMDs are slightly different for force excited and base excited SDOF; however, they have very similar frequency response characteristics. In Figs. 7(a and b), STMDs reduce the response more than their passive counterparts. The passive TMDs lose their efficiency beyond resonance frequency; they have even higher response than "No TMD" case for $\omega/\omega_n < \sim 0.95$ and $\omega/\omega_n > \sim 1.05$. In case the fundamental frequency changes due to damage or deterioration of the main structure then the TMD will be off-tune; hence, it will lose its effectiveness significantly, whereas, the STMD is robust against such changes since it is always tuned to the excitation frequency.

The optimum frequency, damping ratio, and frequency range of passive TMDs in a forced-excited SDOF are computed numerically from the minimum value of curves shown in Figs. 8 and 9.
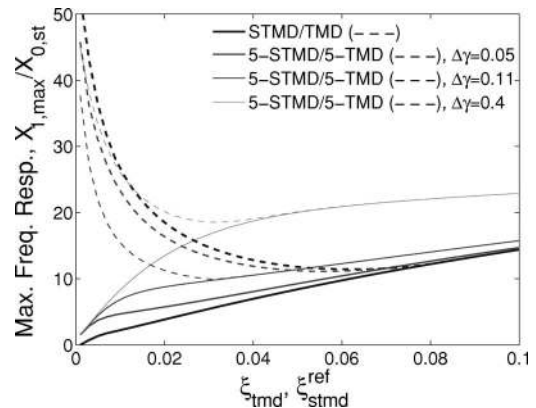

Fig. 9. Maximum frequency response versus TMD damping ratio for force excited SDOF with TMD/STMD and 5TMD (dashed line)/5STMD (solid line)

Table 1. Parameters of Passive and Semiactive TMDs

		Force excitation		Base excitation	
		SDOF	5-DOF	SDOF	5-DOF
μ		0.01	0.0159	0.01	0.0159
TMD (Figs. 7 and 10–25)	γ	0.989	0.982	0.985	0.978
	ξ_{tmd}	0.062	0.079	0.062	0.080
5-TMD (Figs. 7 and 10–25)	γ_c	0.989	0.982	0.985	0.978
	Δ_γ	0.11	0.15	0.12	0.14
	ξ_{tmd}	0.031	0.031	0.023	0.035
21-TMD (Fig. 7)	γ_c	0.989	0.982	0.985	0.978
	Δ_γ	0.15	0.18	0.15	0.18
	ξ_{tmd}	0.019	0.029	0.018	0.026
STMD (Figs. 7 and 10–25)	ξ_{tmd}^{ref}	0.01	0.01	0.01	0.01
5-STMD (Fig. 7)	Δ_γ	0.11	0.15	0.12	0.14
	ξ_{tmd}^{ref}	0.01	0.01	0.01	0.01
5-STMD (Figs. 10–25)	Δ_γ	0.05	0.05	0.05	0.05
	ξ_{tmd}^{ref}	0.01	0.01	0.01	0.01
21-STMD (Fig. 7)	Δ_γ	0.15	0.15	0.15	0.15
	ξ_{tmd}^{ref}	0.01	0.01	0.01	0.01

The corresponding figures for base excited SDOF are essentially the same; therefore are not presented here to avoid duplicity. As seen in both Figs. 8 and 9, passive TMDs have specific optimum damping ratios and frequency ranges whereas STMD decreases the response further as frequency range, $\Delta\gamma$ and reference damping ratio, $\xi_{stmd}^{\mathrm{ref}}$ decrease. Also SMTMD can behave as a single STMD by decreasing the frequency range to zero. Another interesting observation in Fig. 9 is the convergence of maximum frequency response in both passive and semiactive TMDs as damping ratio of TMDs increases.

Time Histories

In order to verify the results in the previous section, SDOF and 5DOF main structures equipped with real-time tuned STMDs are subjected to several force and base excitations; time history responses are computed and compared with passive TMDs. Optimum parameters of passive TMD and 5 TMD used in the following simulations are listed in Table 1.

First, time histories of force excited SDOF and 5DOF structures are studied for harmonic type signals shown in Fig. 6. The fundamental frequency is 2 Hz and fundamental damping ratio is 1% for both SDOF and 5DOF system. Both structures equipped with STMD and 5STMD are compared with their passive counterparts in Figs. 10–15. For 2 Hz harmonic sinusoidal force excitation the dynamic response of SDOF is shown in Fig. 10. Semiactive systems reduce the steady-state response significantly. Similar performance is observed in 5DOF structure in Fig. 11, which shows the normalized maximum steady-state story displacements (normalized with respect to maximum steady-state response of top floor displacement of the original structure without any passive or semiactive TMDs). For harmonic sinusoidal excitation, STMD leads to least response, which is in agreement with results in frequency domain (see Fig. 9). However, it was found that if the excitation frequency is not tracked very accurately, 5STMD becomes more effective as 5STMD tuned within a small frequency range compensates for tracking errors.

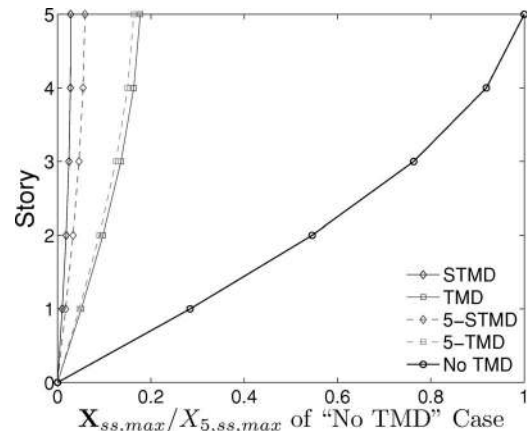Figs. 12 and 13 show the responses of SDOF and 5DOF struc-

Fig. 10. Dynamic response of force excited SDOF main structure (f_n=2 Hz) under harmonic sinusoidal load (f=2 Hz): (a) no TMD, TMD, and STMD; (b) no TMD, MTMD, and SMTMD

Fig. 11. Maximum steady-state response of force excited 5DOF main structure (f_{n1}=2 Hz) under harmonic sinusoidal loading (f=2 Hz) for no TMD, TMD, MTMD, STMD, and SMTMD
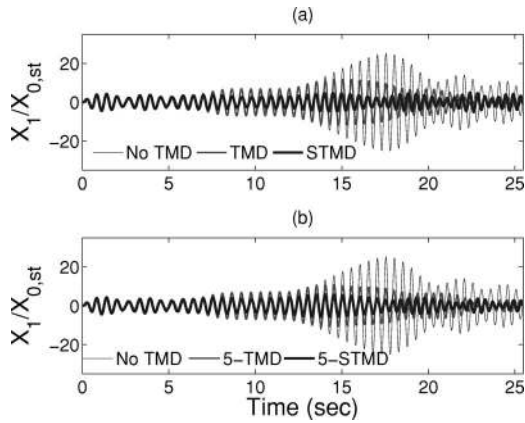
Fig. 12. Dynamic response of force excited SDOF main structure (f_n=2 Hz) under discrete sinusoidal sweep load (1.6 Hz<f <2.4 Hz): (a) no TMD, TMD, and STMD; (b) no TMD, MTMD, and SMTMD
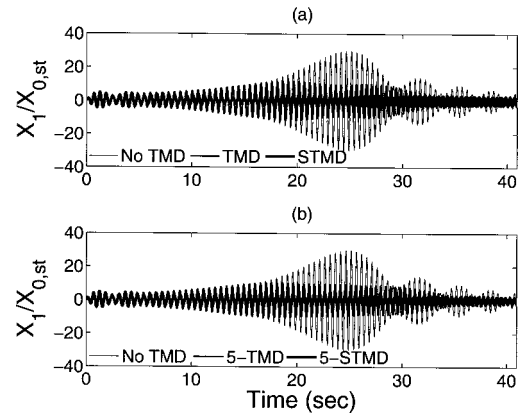

Fig. 14. Dynamic response of force excited SDOF main structure (f_n=2 Hz) under linear chirp load (1.6 Hz<f<2.4 Hz): (a) no TMD, TMD, and STMD; (b) no TMD, MTMD, and SMTMD

ture under discrete sinusoidal sweep load with consecutive ten cycles of five frequencies (1.6, 1.8, 2.0, 2.2, and 2.4 Hz). Fig. 12 presents the normalized maximum transient story displacements (normalized with respect to maximum transient response of top floor displacement of the original structure without any passive or semiactive TMDs). In Fig. 13, 5STMD leads to smaller response than others. 5STMD distributed within a small frequency range is more effective due to the capability to compensate the small errors/delays in frequency tracking in the excitation signal [Fig. 6(b)]. The third harmonic signal is a linear chirp with frequencies varying from 1.6 to 2.4 Hz continuously. The responses shown in Figs. 14 and 15 are similar to discrete sinusoidal sweep case. In linear chirp signal, the excitation frequency changes gradually with time and delay is small. The advantage of whole TMD mass tuned to single frequency in STMD balances with benefit of covering a frequency range in 5STMD. Therefore, in both cases (Figs. 14 and 15) STMD and 5STMD perform almost same.

Time histories clearly prove that excitation frequency of simple harmonic signals can be tracked accurately and semiactive TMDs tuned to excitation frequency with low damping ratios outperforms their passive counterparts. Next, response to narrow

band stationary excitation is evaluated. Therefore, dynamic responses of SDOF and 5DOF structures (with 0.5 Hz fundamental frequency) under a narrow-band force excitation are studied. Fig. 16 shows the excitation signal and its frequency tracking. STFT parameters are selected as: a rectangular window of length, WL=4 s, TL=Δt=0.02 s, AL=1 s, and t_0=3 s. As observed from Figs. 17 and 18, STMDs are superior than passive systems in reducing the response of the force excited SDOF and 5DOF main structures. To investigate the potential of STMDs in nonstationary signals, time history responses of SDOF and 5DOF structures (with 2 Hz fundamental frequency) subjected to first 10 s of the 1940 El Centro Earthquake are computed. The ground acceleration and frequency tracking are shown in Fig. 19. Time step for the acceleration record is 0.01 s. STFT parameters are selected as: a rectangular window of length, WL=1 s, TL=Δt=0.01 s, AL=1 s, and t_0=1.5 s. The main structure response is reduced most by STMD and 5STMD as seen in Figs. 20 and 21, whereas passive TMD and 5TMD increase the response of the main structure.

It is also interesting to study the performance of STMDs when some damage occurs in the main structure. 5DOF main structure subjected to stationary and nonstationary excitations [shown in Figs. 16(a) and 19(b), respectively] is considered. The damage is
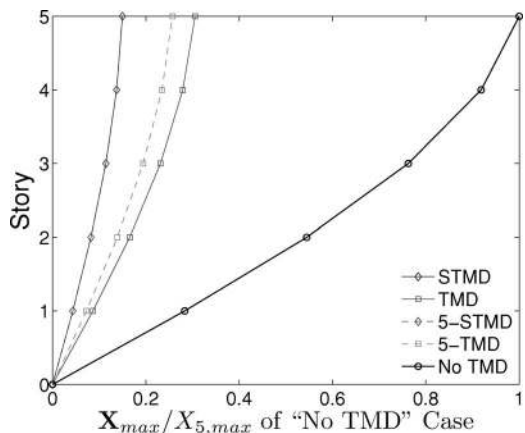

Fig. 13. Maximum transient response of force excited 5DOF main structure (f_{n1}=2 Hz) under discrete sinusoidal sweep loading (1.6 Hz<f<2.4 Hz) for no TMD, TMD, MTMD, STMD, and SMTMD

Fig. 15. Maximum transient response of force excited 5DOF main structure (f_{n1}=2 Hz) under linear chirp loading (1.6 Hz<f <2.4 Hz) for no TMD, TMD, MTMD, STMD, and SMTMD
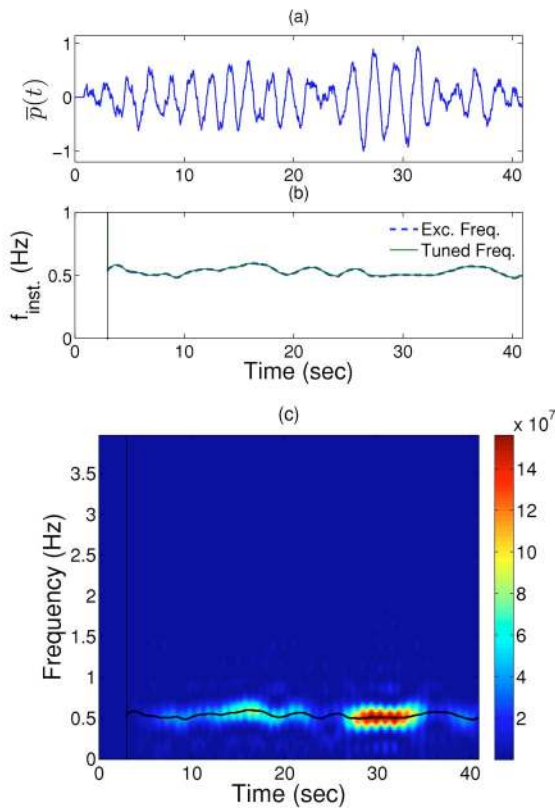
Fig. 16. (a) Narrow band stationary excitation; (b) frequency tracking; and (c) STFT spectrum

modeled such that K_0 reduces to 0.8 K_0 at the first story. Figs. 22 and 23 show the top floor displacement and normalized maximum response of 5DOF structure ($f_{n1}=0.5$ Hz) subjected to stationary excitation presented in Fig. 16(a). The damage is a step function at $t=20$ s. Similarly, Figs. 24 and 25 show the top floor displacement and normalized maximum response of 5DOF structure ($f_{n1}=2$ Hz) subjected to first 10 s of the 1940 El Centro Earthquake presented in Fig. 19(a). The damage is a step function at $t=2.5$ s. In both cases STMDs have superior performance compared to passive ones. STMDs have significant potential against stationary and non-stationary signals as evident from preliminary
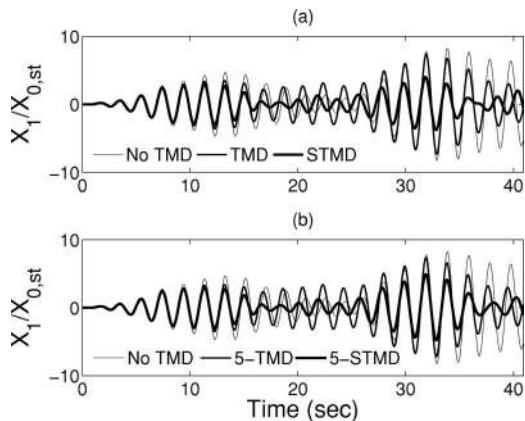
Fig. 17. Dynamic response of force excited SDOF main structure ($f_n=0.5$ Hz) under stationary excitation: (a) no TMD, TMD, and STMD; (b) no TMD, MTMD, and SMTMD
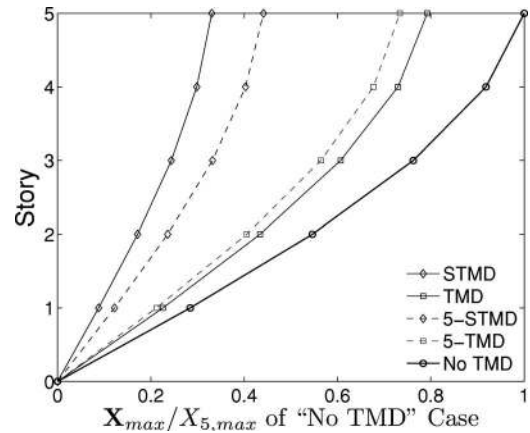
Fig. 18. Maximum transient response of force excited 5DOF main structure ($f_{n1}=0.5$ Hz) under stationary excitation for no TMD, TMD, MTMD, STMD, and SMTMD

simulations presented here. A more extensive study is needed to generalize the results of this study for random excitations.

Conclusions

Performance of semiactive variable stiffness TMD and MTMD systems are evaluated in comparison with their passive counterparts. In the first part, frequency response functions are employed to investigate the behavior and governing parameters of STMD and SMTMD for harmonic forces. In the second part, time histories of SDOF and 5DOF structures equipped with STMD/
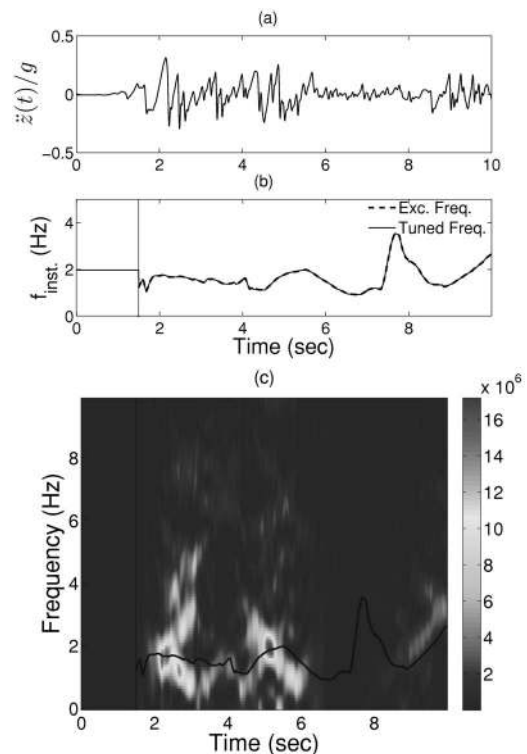

Fig. 19. (a) 1940 El Centro Earthquake; (b) frequency tracking; and (c) STFT spectrum
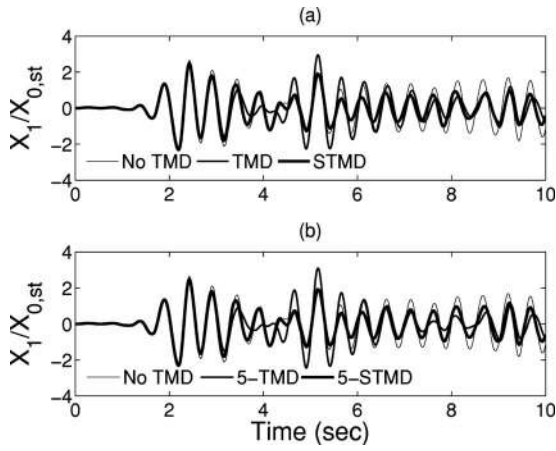
Fig. 20. Dynamic response of base excited SDOF main structure (f_n=2 Hz) under 1940 El Centro Earthquake: (a) no TMD, TMD, and STMD; (b) no TMD, MTMD, and SMTMD
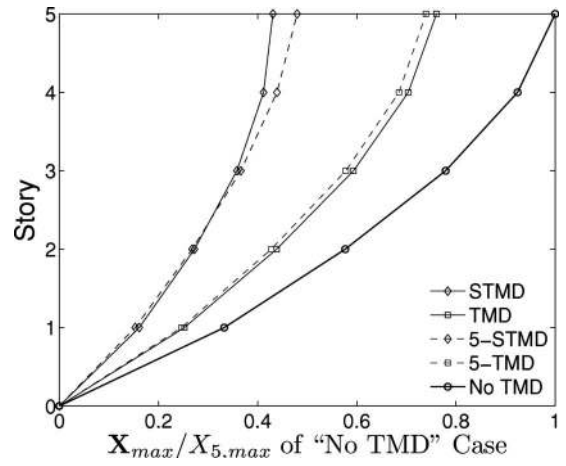

Fig. 23. Maximum transient response of force excited 5DOF main structure (f_{n1}=0.5 Hz) with a step stiffness change under stationary excitation for no TMD, TMD, MTMD, STMD, and SMTMD
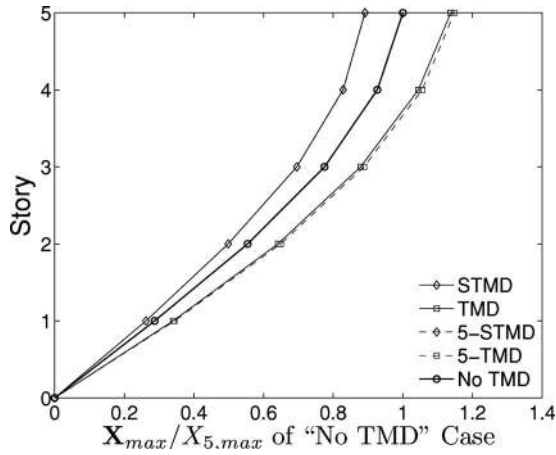

Fig. 21. Maximum transient response of base excited 5DOF main structure (f_{n1}=2 Hz) under 1940 El Centro Earthquake for no TMD, TMD, MTMD, STMD, and SMTMD
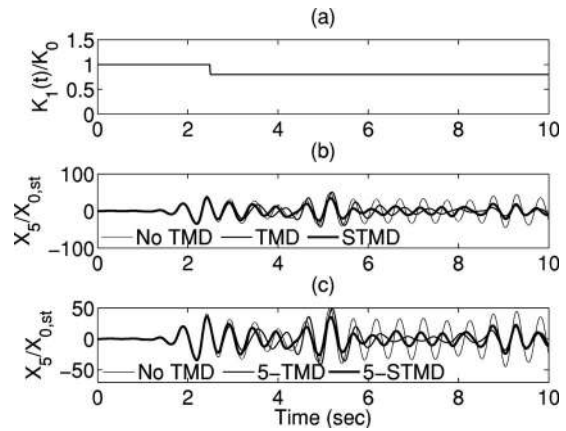
Fig. 24. Top floor displacement of base excited 5DOF main structure (f_{n1}=2 Hz) under 1940 El Centro Earthquake: (a) step stiffness change; (b) no TMD, TMD, and STMD; and (c) no TMD, MTMD, and SMTMD
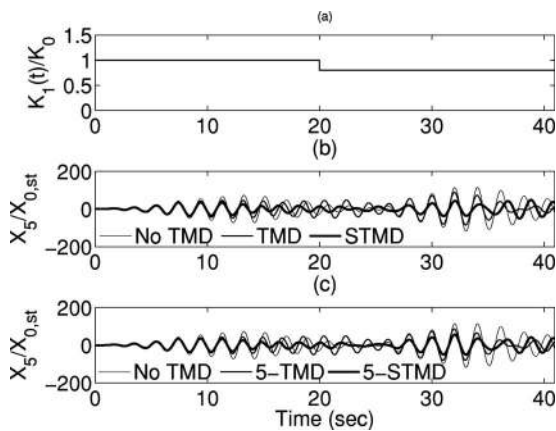

Fig. 22. Top floor displacement of force excited 5DOF main structure (f_{n1}=0.5 Hz) under stationary excitation: (a) step stiffness change; (b) no TMD, TMD, and STMD; and (c) no TMD, MTMD, and SMTMD
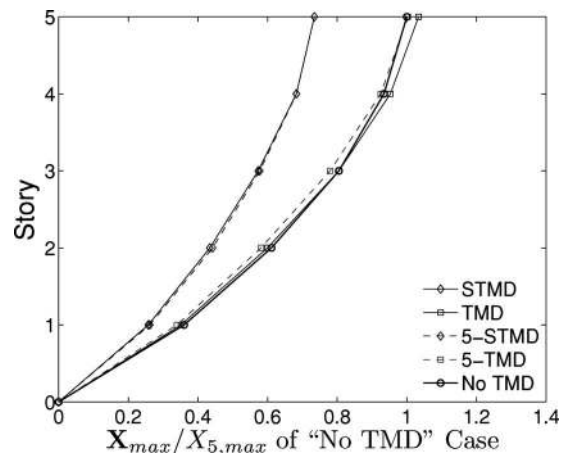

Fig. 25. Maximum transient response of base excited 5DOF main structure (f_{n1}=2 Hz) with a step stiffness change under 1940 El Centro Earthquake for no TMD, TMD, MTMD, STMD, and SMTMD

SMTMD under harmonic, stationary, and non-stationary random excitations (i.e., 1940 El Centro) are computed. The main conclusions of this study are:

1. In this study the STMD frequency has been tuned to the excitation frequency which is found to be very effective; however, in an earlier study by the first writer (Nagarajaiah and Varadarajan 2005) it was shown that it is also effective to tune the STMD frequency to the main structure fundamental frequency.

2. For harmonic signals, if the excitation frequency is known or tracked very accurately, single STMD leads to the least response of the main structure compared to multiple STMDs, since STMD has the advantage of greater mass tuned to exact excitation frequency. But in practice, the excitation frequency is either not known or can be tracked with some error and/or delay. Therefore, multiple STMDs distributed within a small frequency range may be more effective due to the capability to compensate the small errors/delays in frequency tracking and/or randomness in the excitation signal. If the SMTMD frequency range is increased further, its effectiveness would decrease because of distributing the mass away from the resonance frequency and STMD would be superior again in agreement with results of parametric study.

3. SMTMD can also behave as a single STMD in real time by reducing the frequency range to zero. They can be tuned as a single STMD depending on the time-frequency characteristics of the excitation signal. The redundancy in SMTMD makes it more reliable in the sense that if one STMD fails, the rest can be readjusted instantaneously.

4. MTMD has an optimum frequency range and an optimum damping ratio for a given number of TMDs. Once the number of TMDs is decided and optimum values of the frequency range and damping ratio can be found for the design of MTMD. In case of SMTMD, there are no specific optimum values. The lower the damping ratio and the frequency range, the better performance SMTMD will have.

5. STMD and SMTMD are more robust against changes in individual TMD damping ratio and changes in main structure natural frequency compared to passive TMD and MTMD. This is observed both in frequency domain and time domain responses.

6. Based on the limited study with stationary and nonstationary excitations presented in this study, STMDs are able to reduce the response of the main structure whereas passive TMDs may increase it, indicating their potential. A more extensive study is needed to generalize the results of this study for random excitations.

Acknowledgments

References

Abe, M. (1996). "Semi-active tuned mass dampers for seismic protection of civil structures." *Earthquake Eng. Struct. Dyn.*, 25(7), 743–749.

Abe, M., and Fujino, Y. (1994). "Dynamic characterization of multiple tuned mass dampers and some design formulas." *Earthquake Eng. Struct. Dyn.*, 23(8), 813–835.

Abe, M., and Igusa, T. (1995). "Tuned mass dampers for structures with closely spaced natural frequencies." *Earthquake Eng. Struct. Dyn.*, 24(2), 247–261.

Abe, M., and Igusa, T. (1996). "Semi-active dynamic vibration absorbers for controlling transient response." *J. Sound Vib.*, 198(25), 547–569.

Bobrow, J., Jabbari, F., and Thai, K. (2000). "A new approach to shock isolation and vibration suppression using a resetable actuator." *J. Dyn. Syst., Meas., Control*, 122(3), 570–573.

Cohen, L. (1995). *Time-frequency analysis*, Prentice-Hall, Englewood Cliffs, N.J.

Den Hartog, J. P. (1985). *Mechanical vibrations*, Dover, New York.

Hrovat, D., Barak, P., and Rabins, M. (1983). "Semi-active versus passive or active tuned mass dampers for structural control." *J. Eng. Mech.*, 109(3), 691–705.

Igusa, T., and Xu, K. (1994). "Vibration control using multiple tuned mass dampers." *J. Sound Vib.*, 175(4), 491–503.

Kareem, A., and Kline, S. (1995). "Performance of multiple mass dampers under random loading." *J. Struct. Eng.*, 121(2), 348–361.

Kaynia, A. M., Biggs, J. M., and Veneziano, D. (1981). "Seismic effectiveness of tuned mass dampers." *J. Struct. Div.*, 107(8), 1465–1484.

Kobori, T., and Takahashi, M. (1993). "Seismic response controlled structure with active variable stiffness system." *Earthquake Eng. Struct. Dyn.*, 22(12), 925–941.

McNamara, R. J. (1977). "Tuned mass dampers for buildings." *J. Struct. Div.*, 103(9), 1785–1798.

Nagarajaiah, S., and Mate, D. (1998). "Semiactive control of continuously variable stiffness system." *Proc., 2nd World Conf. Struct. Control*, Vol. 1, Kyoto, Japan, 397–405.

Nagarajaiah, S., and Varadarajan, N. (2000). "Novel semiactive variable stiffness tuned mass damper with real time tuning capacity." *Proc., 13th Engineering Mechanics Conf.* (CD-ROM), ASCE, Reston, Va.

Nagarajaiah, S., and Varadarajan, N. (2005). "Short time Fourier transform algorithm for wind response control of buildings with variable stiffness tmd." *Eng. Struct.*, 27(3), 431–441.

Nagarajaiah, S., Varadarajan, N., and Sahasrabudhe, S. (1999). "Variable stiffness and instantaneous frequency." *Proc., World Structures Congress*, ASCE, Reston, Va., 858–861.

Sladek, J. R., and Klingner, R. E. (1983). "Effect of tuned-mass dampers on seismic response." *J. Struct. Eng.*, 109(8), 2004–2009.

Spencer, B. F., and Nagarajaiah, S. (2003). "State-of-the-art of structural control." *J. Struct. Eng.*, 129(7), 845–856.

Sun, J. Q., Jolly, M. R., and Norris, M. A. (1995). "Passive, adaptive, and active tuned vibration absorber—A survey." *Trans. ASME*, 117, 234–242.

Varadarajan, N., and Nagarajaiah, S. (2004). "Wind response control of building with variable stiffness tuned mass damper using empirical mode decomposition/hilbert transform." *J. Eng. Mech.*, 130(4), 451–458.

Warburton, G. B. (1981). "Optimum absorber parameters for minimizing vibration response." *Earthquake Eng. Struct. Dyn.*, 9(3), 251–262.

Xu, K., and Igusa, T. (1992). "Dynamic characteristics of multiple substructures with closely spaced frequencies." *Earthquake Eng. Struct. Dyn.*, 21(12), 1059–1070.

Yamaguchi, H., and Harnpornchai, N. (1983). "Fundamental characteristics of multiple tuned mass dampers for suppressing harmonically forced oscillations." *Earthquake Eng. Struct. Dyn.*, 22(1), 51–62.

Yang, J. N., Kim, J. H., and Agrawal, A. K. (2000). "Resetting semiactive stiffness damper for seismic response control." *J. Struct. Eng.*, 126(12), 1427–1433.